

L183, a Quiescent Core?

Jian-Jun Zhou^{1,2}, Xing-Wu Zheng^{1*} and Yu-Xi Chen¹

¹ Department of Astronomy, Nanjing University, Nanjing 210093

² Urumqi Astronomy Observatory, Chinese Academy of Science, Xingjiang 830011

Received 2001 January 15; accepted 2001 April 13

Abstract Some observed results of NH_3 (1,1) and (2,2) line emission in the starless dark cloud L183 are reported. Our observation suggests that the dense core of L183 has a size of $\sim 0.16 \text{ pc} \times 0.1 \text{ pc}$ with a mass of $\sim 12 M_\odot$. A velocity gradient of $4 \text{ km s}^{-1} \text{ pc}^{-1}$ from the north to the south was detected. The velocity shift corresponds to a central mass of $\sim 5 M_\odot$. If it is caused by rotation, the mass would be much less than the value above. This suggests that there may be more mass in the envelope of L183 than in the central region. The analysis of our data and the evidence in the literature about L183 indicate that it may be undergoing a process of collapsing to form a low-mass binary dense core.

Key words: ISM: clouds — Stars: formation — Stars: low-mass

1 INTRODUCTION

L183 is a prototype dark cloud core. It lies in a relatively isolated region of the sky at a distance of 160 pc (Snell et al. 1981). No internal infrared source was found (Sargent 1983, IRAS Point Source Catalogue 1985). Therefore, L183 is a good sample to study the formation of low mass stars. There are many species of molecules in L183, including H_2CO (Evans & Kutner 1976); DCO^+ , N_2D^+ , DCN and DNC (Turner & Zuckerman 1978); ^{12}CO and ^{13}CO (Caldwell 1979); H_2CO^+ (Guélin Langer & Wilson 1982); CS (Snell, Langer & Frerking 1982); C^{18}O , CS , H^{13}CO^+ , SO , NH_3 , C_3H_2 (Swade 1989a, b). L183 comprises a less dense envelope and a dense core (Swade 1989a, b), in which there are two compact cores seen in the contour map of NH_3 (1,1) main line ($\alpha = 15^{\text{h}}51^{\text{m}}30^{\text{s}}$, $\delta = -02^\circ43'31''$; $\alpha = 15^{\text{h}}51^{\text{m}}30^{\text{s}}$, $\delta = -02^\circ40'31''$) (Ungerechts et al. 1980; Swade 1989a, b). They display a definite north-south elongation. The total mass of L183 is $\sim 190 M_\odot$ and the core has about a few tens solar mass. (Myers et al. 1983, Benson & Myers 1989, Swade 1987, 1989). Observations suggested that the dense core shows a kinetic temperature of 12 K and a peak molecular hydrogen density $3 \times 10^4 \text{ cm}^{-3}$ (Swade 1989).

The purpose of our program is to get evidence for the collapse of dense cores in starless dark clouds. We give a description of the observation in Section 2, and the results of observation and data reduction in Section 3. Our analysis and tentative conclusion are given in Section 4.

* E-mail: xwzheng@nju.edu.cn

2 OBSERVATIONS AND DATA REDUCTION

The observations were carried out at the National Radio Astronomy Observatory at Greenbank, West Virginia, U.S.A., using the 43-m radio telescope during March 15–19 of 1999. At the observing frequency (23 GHz) the telescope's half-power beam width is about $77''$ and the main beam efficiency is 0.45. The observing bandwidth was 5 MHz. The spectrometer for the observations was the model IV autocorrelator with 256 channels that provide an effective resolution of 19.5 kHz corresponding to 0.25 km s^{-1} . The $(J, K) = (1, 1)$ and $(2, 2)$ are observed simultaneously at the frequency-switching mode. Both the left circular polarization and right circular polarization components were fed into the correlator and combined during the reduction. Observations were obtained in a 7×5 grid with positions uniformly spaced at 90 intervals. The integration time is 0.3 minutes.

The peak flux intensity, FWHM and line central velocity were fitted using the software UNIPOPS. The initial data were corrected by a Gaussian model for all appeared hyperfine components.

3 RESULTS

We calculate the optical depth, excitation temperature, rotational temperature, column density and number density following P. T. Ho (1977). The results of calculation are listed in Table 1.

Table 1

Position Offset	Optical Depth	Excitation Temperature	Column Density	Rotational Temperature	Number Density
(1.5', 3')	0.471040	5.274987	1.129596e+014	10.217935	10080.436849
(0, 3')	1.393338	5.210799	3.29615e+014	12.217505	9696.776855
(1.5', 1.5')	2.984104	3.302454	4.188107e+014	14.740557	1658.669220
(1.5', 4.5')	1.230422	3.932443	2.116896e+014	10.056752	3750.306688
(0, 4.5')	0.943388	3.865483	1.591241e+014	10.508790	3507.408485
(-1.5', 3')	0.758751	4.185126	1.402042e+014	10.746959	4717.617737
(-1.5', 4.5')	1.652506	3.205991	2.239189e+014	11.212918	1373.004445
(-1.5', 1.5')	1.548261	3.603200	2.407057e+014	9.922579	2605.306903
(-3', 3')	2.865016	3.154865	3.808641e+014	10.382687	1224.912513
(0, 0)	1.423928	5.363630	3.541940e+014	8.215363	10627.769194
(-1.5', 0)	1.102841	4.281361	2.091386e+014	9.71359	5108.621045
(1.5', 0)	1.400414	4.386867	2.730224e+014	8.915535	5552.765308
(0, -1.5')	0.386044	6.566826	1.178007e+014	9.657043	20855.966609
(0, 1.5')	1.487022	5.268761	3.561333e+014	11.051165	10042.769925
(-1.5', -1.5')	0.992906	3.654319	1.569197e+014	10.668053	2775.226121
(1.5', -1.5')	0.833705	4.886707	1.835746e+014	9.344638	7906.984028
(0, -3')	0.207771	7.475290	7.295656e+013	10.126831	35042.174425
(1.5', -3')	0.382454	5.541029	9.685925e+013	13.793272	11788.579762
(3', -3')	1.088608	3.290719	1.521413e+014	11.731586	1623.471105
(1.5', -4.5')	1.505408	3.196544	2.032727e+014	11.613761	1345.469327
(0, -4.5')	1.430657	3.327547	2.025924e+014	10.773189	1734.351146
(3', -4.5')	2.102458	2.999120	2.630673e+014	12.028125	787.333759

The position offset is reckoned from ($\alpha = 15^{\text{h}}51^{\text{m}}30^{\text{s}}$ $\delta = -02^{\circ}43' 52''$)

Fig. 1 shows one typical spectrum of NH_3 (1, 1). No hyperfine structures of satellite lines are detected except the inner left satellite line due to low velocity resolution in our observations. The dips are artifacts of the frequency switching mode. Fig. 2 displays all the spectra we obtained according to their relative position. The position offsets refer to the peak of NH_3 (1, 1) emission ($\alpha = 15^{\text{h}}51^{\text{m}}30^{\text{s}}$ $\delta = -02^{\circ}43' 52''$). Fig. 3 shows the spatial contour map of the NH_3 (1, 1) emission at velocity $\sim 2.58 \text{ km s}^{-1}$. In Fig. 4 we have plotted an integrated map from velocity ~ 2.2 to $\sim 2.96 \text{ km s}^{-1}$. These two maps illustrate two observed features of the dense core. (1) There is only one peak detected at the position $\alpha = 15^{\text{h}}51^{\text{m}}30^{\text{s}}$ $\delta = -02^{\circ}43' 52''$ in our maps. (2) The spatial distribution of the dense core displays a definite elongation from north to south. It appears to be consistent with the previous observation of Ungerechts et al. (1980). The dense core extends along the major axis $\sim 0.16 \text{ pc}$ and the minor axis is $\sim 0.1 \text{ pc}$ (at an assumed distance of 160 pc). The position-velocity (PV) map constructed from spectra observed along the major axis of the dense core is displayed in Fig. 5. The map reveals a velocity field. Between $\sim 1.65 \text{ km s}^{-1}$ to $\sim 2.3 \text{ km s}^{-1}$, two velocity features or components can be identified. These two components correspond to two individual cores. In the PV map we found a slight systematic shift. We will discuss in more detail in the following section.

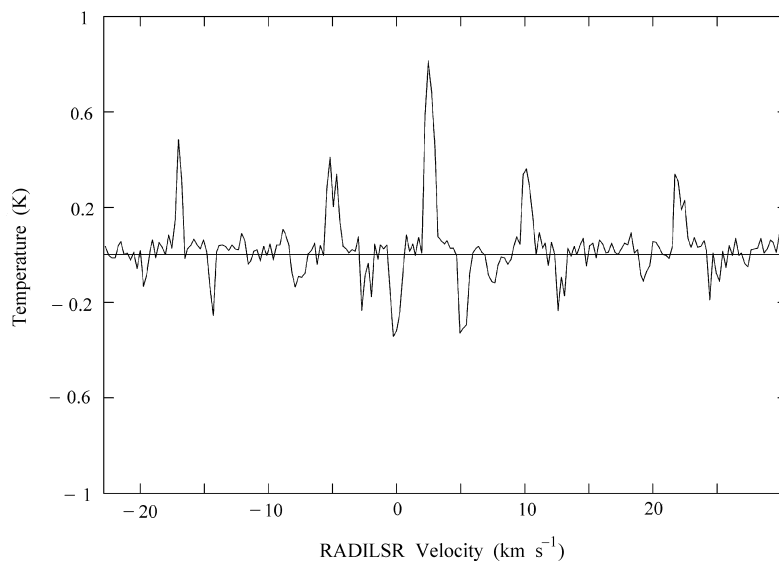


Fig. 1 NH_3 (1, 1) spectrum of L183 at position ($\alpha = 15^{\text{h}}51^{\text{m}}31^{\text{s}}$, $\delta = -02^{\circ}45' 22''$), the velocity resolution of it is 0.25 km s^{-1} . Main line and four satellite lines are shown clearly. The dips of the spectrum are the artifacts of the frequency-switching mode.

4 DISCUSSION

The key stage of star formation is when the molecular cloud becomes unstable and starts to collapse. So it is necessary to know whether the dark cloud core of L183 is stable or not. From our observations we estimate the dark cloud core to have a mass of $15 M_{\odot}$ including the

mass of He. The result is consistent with previous results such as $\sim 15 M_{\odot}$ (Swade 1987), $\sim 21 M_{\odot}$ (Myers et al. 1983) and $29 M_{\odot}$ (Benson & Myers 1989). By balancing the thermal and gravitational energies we obtain a Virial mass of the dense core of $\sim 8 M_{\odot}$. It is obvious that thermal pressure alone cannot support against the gravity. If such a core (with $n \sim 10^4 \text{ cm}^{-3}$) is prevented from collapsing by the support of magnetic field, a magnetic field $B \sim [5 \times 10^{-5} n^2 (M/M_{\odot})]^{1/3} \sim 42 \mu\text{G}$ would be required (Spitzer 1978). It is obvious we cannot determine whether or not L183 is quiescent without knowing the exact value of the magnetic field. But it is natural for us to imagine that the molecular cloud has been there for a long time and that the field has decayed compared with the initial state. So the core may be collapsing slowly.

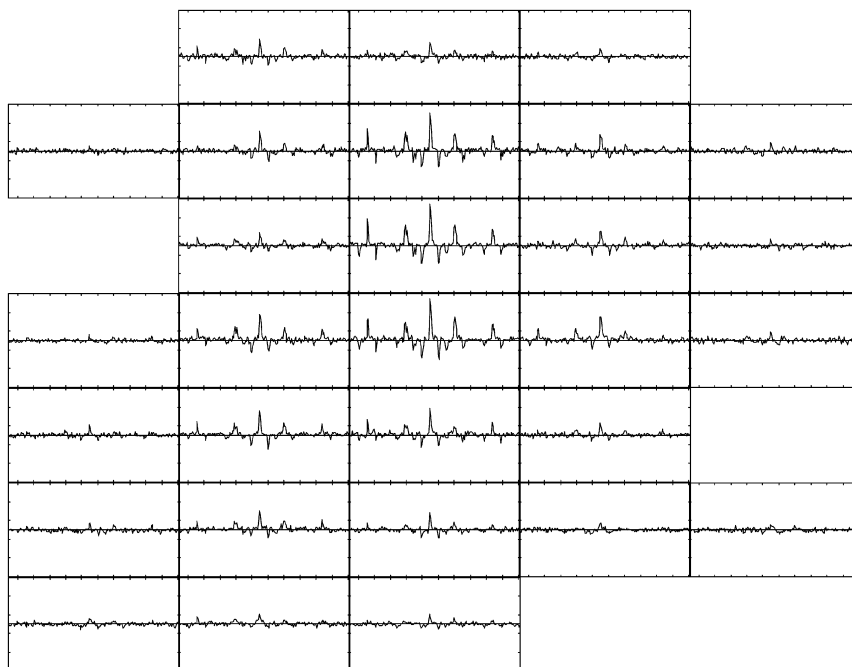


Fig. 2 All spectra of $\text{NH}_3(1, 1)$ of L183 are displayed according to their relative position. The profile of the dense core of L183 appears on it. The description of each spectral is the same as that in Fig. 1.

In our Fig. 5, a velocity shift can obviously be seen. If the velocity shift was caused by rotation of the dense core, then the measurement suggests that the core of L183 has a rotation velocity of $\sim 0.32 \text{ km s}^{-1}$, which corresponds to a central mass of $\sim 5 M_{\odot}$, much less than our estimation of the core mass mentioned above. This suggests that there may be more mass in the envelope of L183 than in the central region. Though the blue-shift and red-shift may result from some other mechanism, the rotation seems to be a reasonable explanation.

The molecular lines provide us with another criterion for deciding whether a cloud core is collapsing or not (Zhou et al. 1992, 1993, 1994). The basic signatures of a collapsing core, for a spherical symmetry and centrally peaked density distribution are: 1) The line width increases

with increasing critical density of the line. 2) Optically thin lines should appear symmetric while optically thick lines are skewed to the blue and in some case have an absorption dip at the rest velocity of the cloud (Zhou et al. 1994b). Fortunately, there are many spectra of L183

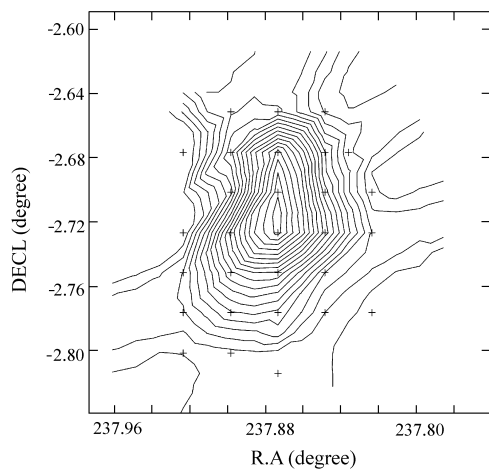


Fig. 3 Contour map of the main beam line brightness temperature at the peak of the main line of $\text{NH}_3(1, 1)$. The crosses denote observing positions. The intensity declines outward. The first level is 0.12 K and the increment is 0.03 K.

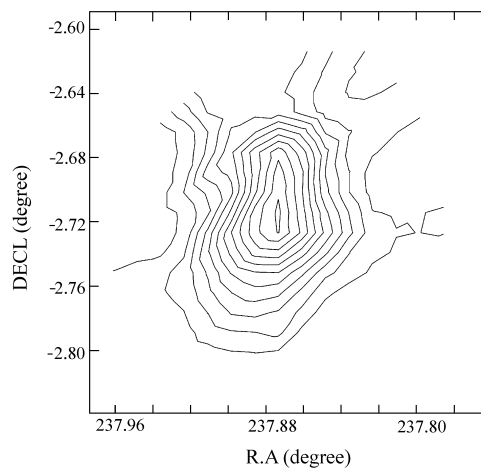


Fig. 4 Contour map of the integrated main beam line brightness temperature at the peak of the main line of $\text{NH}_3(1, 1)$. The first level and the increment both are 35 K km s^{-1} .

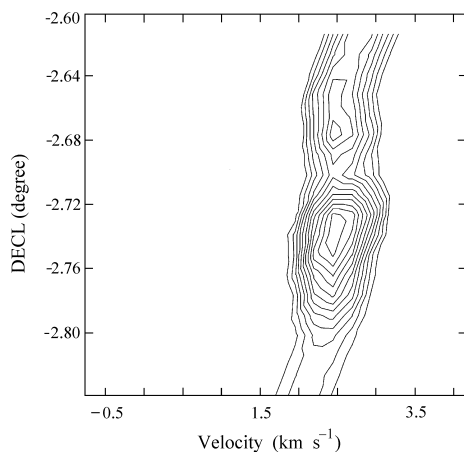


Fig. 5 The position-velocity map of L183, which indicates that L183 consists of two more dense cores. There is a velocity gradient of $4 \text{ km s}^{-1} \text{ pc}^{-1}$ from north to south. The blueshift and redshift may result from rotation.

in the literature. For example, the spectra of $C^{18}O$ ($J = 1 - 0$) shown in the figure 6 of the paper of Swade (Swade 1989) exhibit obvious redshifted line wings in the panels a, b, c, d and f; the spectra of CS ($J = 2 - 1$) shown in the figure 7 of the same paper show redshift and absorption dips in the panel b, c and d at the rest velocity of the cloud; the spectra of SO ($J = 2, 3 - 1, 2$) in the same paper also show evidence of redshift. The spectra of NH_3 (1, 1) (2, 2) C_3H_2 ($1_{10} - 1_{01}$) are very narrow and symmetric. We can see clearly that optically thin lines are symmetric, while optically thick lines show obvious redshift in the figure 4 of the paper of Swade et al (1992), which is obtained in the vicinity of one dense core of L183. All these spectra are consistent with the second signature of collapsing dense core, they are the critical evidence of collapse. However, they are not consistent with the first signature of collapsing core. This may be due to that there is no infrared source in the center of L183.

The theory of star formation (Shu 1987) suggests that in the initial state the molecular cloud can support against the self-gravity with the help of magnetic field. The magnetic forces provide indirect support to the neutrals against their self-gravity via the intermediary of fractional drag in the process of ambipolar diffusion (Mestel and Spitzer 1956). But the equilibrium state cannot remain forever. In time the magnetic field tends to decay, and the molecular cloud has to adjust its size and shape so as to support against the self-gravity by thermal pressure alone. This automatically leads to a mechanism for the formation of substructures (cores and envelopes) in molecular clouds. There are two possibilities: if $M_{cl} > M_{cr}$, cloud evolution is characterized by magnetically diluted collapse (Scott and Black 1980); if $M_{cl} < M_{cr}$, cloud evolution is most likely driven by ambipolar diffusion (Nakano 1979). Here $M_{cl} \sim B^2 R / 4\pi\rho G$, $M_{cr} \sim 10^3 M (B/30\mu G)(R/2pc)^2$, M , B , R and ρ represent mass, magnetic field, radius and density respectively. In general, the magnetic fields in molecular clouds are $\sim 100\mu G$, we have $M_{cl}/M_{cr} \sim 3 \times 10^{-6}$ for L183, so it is probable the formation of its dense core is driven by ambipolar diffusion.

The preceding discussion of the mass of the core, the spectral profiles of several molecules and the theory of star formation all indicate that L183 is probably not a quiescent core. It may be collapsing slowly to form more compact cores via ambipolar diffusion, which may become low-mass binary stars in future. Of course, there are some uncertainties because of our low spatial and velocity resolution, this result needs further testing. Observation with high spatial and velocity resolution is required in the future.

Acknowledgements We thank Professor Ji Yang for providing a good working condition and Ph.D. Jiang Zhibo, Mao Ruiqin for their help and instructive discussion.

References

- Black D. C., Scott E. H., 1983, ApJ, 263, 696
- Benson P. J., Myers P. C., 1989, ApJS, 71, 89
- Caldwell J. A. R., 1979, A&A, 71, 255
- Evans N. J., Kutner M. L., 1976, ApJ, 204, L131
- Guélinln M., Langer W. D., Wilson R. W., 1982, A&A, 107, 107
- Ho P. T. P., 1977, PhD thesis
- IRAS Point Source Catalogue, Joint IRAS Science Group, (Washington, DC: US Government Printing Office)
- Mestel L., Spitzer L., 1956, MNRAS, 116, 503
- Myers P. C., Linke R. A., Benson P. J., 1983, ApJ, 264, 517
- Nakano T., 1979, PASJ, 31, 697

- Sargent A. I., Van Duinen R. J., Nordh H. L. et al., 1983, *AJ*, 88, 88
Scott E. H., Black D. C., 1980, *ApJ*, 239, 166
Shu F. H., 1983, *ApJ*, 273, 202
Shu F. H., 1987, *AR&A*, 25, 23
Snell R. L., Langer W. D., Frerking M. A., 1982, *ApJ*, 255, 149
Spitzer L., 1978, *Physical Processes in the Interstellar Medium*, New York Wiley-Interscience Swade D. A.,
1987, PhD paper
Swade D. A., 1989, *ApJ*, 345, 828
Swade D. A., 1989, *ApJS*, 71, 219
Swade D. A., Schloerb F. P., 1992, *ApJ*, 392, 543
Turner B. E., Zuckerman B., 1978, *ApJ*, 225, L75
Ungerechts H., Walmsley C. M., Winnewisser G., 1980, *A&A*, 88, 259
Walmsley C. M., Winnewisser G., Toelle F., 1980, *A&A*, 81, 245
Wang Y. S., Evans N. J., Zhou S. D., Clemens D. P., 1994, *ApJ*, 454, 217
Zhou S. D., 1992, *ApJ*, 394, 204
Zhou S. D., Evans N. J., Kömpe C., Walmsley C. M., 1993, *ApJ*, 404, 232
Zhou S. D., Evans N. J., Wang Y. S. et al., 1994, *ApJ*, 433, 131